Lunar and Planetary Science XII
Supplement A

Abstracts Presented at a Session of the Twelfth Lunar and Planetary Science Conference March 17, 1981

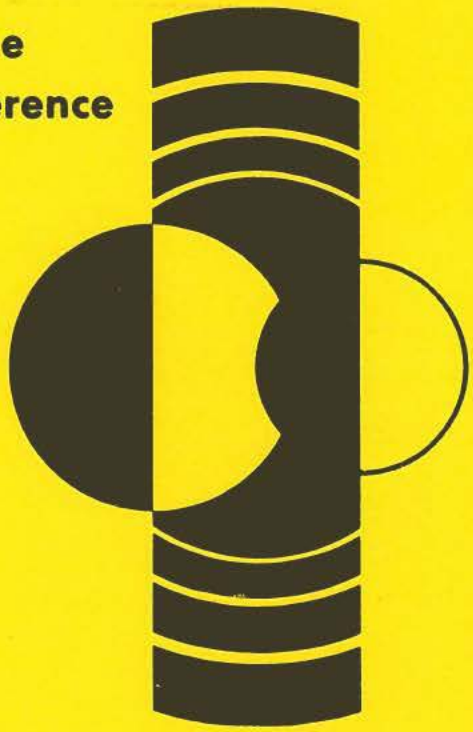

Satellites of Saturn

NASA
National Aeronautics and Space Administration

Lyndon B. Johnson Space Center
Houston, Texas 77058

LPI/USRA
LUNAR AND PLANETARY INSTITUTE
UNIVERSITIES SPACE RESEARCH ASSOCIATION

LUNAR AND PLANETARY SCIENCE XII

SUPPLEMENT A

SATELLITES OF SATURN

ABSTRACTS PRESENTED AT A SESSION OF THE
TWELFTH LUNAR AND PLANETARY SCIENCE CONFERENCE
17 MARCH 1981

Compiled by the
Lunar and Planetary Institute
3303 NASA Road 1
Houston, Texas 77058

LPI Contribution 428

TABLE OF CONTENTS

EVOLUTION OF THE SATURNIAN SATELLITES: THE ROLE OF IMPACT. E. M. Shoemaker and R. F. Wolfe, U.S. Geological Survey, Flagstaff, AZ 86001

The craters observed on the satellites of Saturn have been created by impact of several classes of solid objects, including cometary nuclei and fragments of nuclei, planetesimals, secondary debris ejected from the satellites themselves, and probable collisional debris from coorbiting smaller satellites.

Over the past 3 b.y., cometary nuclei and secondary debris from the satellites have been the principal impacting projectiles. Three classes of comets have contributed to the cratering in the Saturn system: (1) long period, (2) Jupiter family, and (3) Saturn family. The contribution of long-period comets can be estimated by extrapolating from the flux of long-period comets observed in the neighborhood of the Earth. In this extrapolation we assume that the perihelion distances of long-period comets are uniformly distributed between 1 AU and the orbit of Saturn, as predicted by theory (Oort, 1950; Weissman, 1977). Collision probabilities, velocities of impact, masses of cometary nuclei, and cratering rates were estimated by the methods of Shoemaker and Wolfe (1981), the radii of the satellites were determined from Voyager 1 images (Smith et al., 1981), and the distributions of the orbital elements of long-period comets compiled by Marsden (1979) were used in the calculation. The resulting collision parameters and cratering rates for Mimas, Tethys, Dione, and Rhea are listed in Table 1.

Jupiter-family comets include comets that have orbits like those of observed comets with periods less than 20 years and comets that have orbits with Tisserand invariants comparable to those of observed short-period comets but with perihelion distances extending out to 6 AU. As with the long-period comets, the perihelion distribution of Jupiter-family comets is assumed to be uniform between 1 and 6 AU. Following Shoemaker and Wolfe (1981), one-third of the Jupiter-family comets are assumed to be active, and two-thirds to be extinct comets of asteroidal appearance; (944) Hidalgo is considered to be the largest extinct comet. Because only about 10 percent of the Jupiter-family comets cross the orbit of Saturn, they play a very minor role in cratering on the Saturnian satellites (Table 1).

In addition to the long-period and Jupiter-family comets, there is a relatively steady population of cometary nuclei that have been captured into comparatively short period orbits by repeated encounters with Saturn. Because most of these bodies remain too far from the Sun to show detectable cometary activity, their existence is inferred almost entirely from dynamical arguments (Everhart, 1977). (2060) Chiron is the only apparent member of this Saturn family of cometary nuclei so far discovered. We estimate the population of such comets to be about 10^4 bodies larger than 1 km in diameter. Preliminary study of a set of plausible orbits for Saturn-family comets suggests that these objects dominate the present cratering on Mimas, Tethys, Dione, and Rhea (Table 1).

The estimated present rate of creation of craters 10 km in diameter and larger is about 7 times higher on Mimas than on Rhea (Table 1), owing to a combination of higher concentration of cometary flux at the orbit of Mimas than at the orbit of Rhea, higher impact velocities at the orbit of Mimas, and creation of larger craters (for a given impact energy) at the low surface gravity of Mimas. The estimated present rate of creation of craters by cometary impact on Mimas is about equal to the present cratering rate estimated by Shoemaker and Wolfe (1981) for the Galilean satellite Ganymede. Backward extrapolation in time of the estimated present cratering rates suggests that most craters observed on Mimas, Tethys, Dione, and Rhea cannot

have been created by a steady flux of comets over geologic time. Instead, most of these craters probably date from a period of heavy bombardment by planetesimals early in the history of the Saturn system.

Because of the comparatively low surface gravities and low escape velocities on all the Saturnian satellites except Titan, secondary fragments ejected from primary impact craters must create numerous fairly low velocity secondary impact craters on these satellites. On Mimas, for example, the escape velocity is only 0.16 $km \cdot s^{-1}$. Nearly all the material that forms the continuous ejecta blanket of crater Copernicus on the Moon was ejected at velocities exceeding the escape velocity on Mimas. Thus, from each primary impact crater on Mimas a relatively large volume of weakly shocked debris must have been ejected into independent orbits about Saturn. Because most of these orbits would have had semimajor axes close to that of Mimas and only moderate eccentricities, the debris must have been quickly swept up again by collisions with Mimas to form many low-velocity impact craters. The escape velocities on Dione and Rhea are 0.50 and 0.65 $km \cdot s^{-1}$, respectively. Most of the fragments that created the secondary craters surrounding Copernicus on the Moon were ejected at velocities exceeding the escape velocities on Dione and Rhea. Additionally, material ejected at the velocities of the debris that forms the continuous ejecta blanket of Copernicus is scattered globally from primary craters on Dione and Rhea. This scattered debris created many additional secondary craters. We note that, because primary craters are created preferentially on the leading hemisphere of each satellite, most of the escaping secondary debris must be launched with a component of motion directed forward relative to the orbital motion of the satellite. Thus, as this debris is swept up, it collides preferentially on the trailing hemisphere of the satellite.

We interpret the observed population of 10- to 20-km-diameter craters on Mimas (population II of Smith et al., 1981) to consist chiefly of secondary craters. Many of the ~10-km-diameter craters probably are secondaries associated with a 135-km-diameter primary situated near the apex of Mimas. The number of ~20-km-diameter craters, however, is much too large for these craters to be related to this primary crater. Most of the 20-km-diameter craters probably were formed earlier, by impacts of secondary fragments ejected from a still larger primary crater. This larger primary probably exceeded the critical size for disruption of Mimas, and its formation may have led to considerable reorganization of material in the body of Mimas and partial or complete resurfacing of the satellite. This event apparently occurred near the end of the period of heavy bombardment, possibly about 4 b.y. B.P.

We also interpret the population II craters observed on a cratered plain on the leading hemisphere of Dione (Smith et al., 1981) to consist predominantly of secondaries. Here, however, the impacting secondary fragments may have been derived by disruption of a small coorbiting satellite, such as the object recently discovered near a Trojan point in Dione's orbit.

References

Everhart, E. (1977) In Comets Asteroids Meteorites, U. Toledo Pr., 99-104.

Marsden, B. G. (1979) Catalog of Cometary Orbits, Smithsonian Ast. Obs., 88 p.

Oort, J. H. (1950) Bull. Astr. Inst. Netherlands 11, 91-110.

Shoemaker, E. M. and Wolfe, R. F. (1981) In Satellites of Jupiter, U. of Arizona Press (in press).

Smith, B. A. et al. (1981) Voyager 1 Encounter with Saturn, Science (in press).

Weissman, P. R.(1977) In Comets Asteroids Meteorites. U. Toledo Pr., 87-91.

Table 1. Cometary collision parameters and cratering rates to 10-km diameter

Parameter	Comet Class	Mimas	Tethys	Dione	Rhea
U	Long period	1.50	1.55	1.57	1.60
	Jupiter family	.44	.44	.44	.44
	Saturn family	0.27	0.27	0.27	0.27
v_i(km s^{-1})	Long period	25.3	22.3	21.1	19.9
	Jupiter family	20.7	16.7	14.9	12.8
	Saturn family	20.4	16.3	14.5	12.3
F	Long period	14.1	10.1	8.7	7.3
	Jupiter family	31.2	19.9	15.7	11.5
	Saturn family	126	79	62	44
D (km)	Long period	90.9	73.4	66.4	62.5
	Jupiter family	80.9	61.4	54.2	48.4
	Saturn family	80.3	61.2	53.3	47.4
P_c (10^{-13} rev^{-1})	Long period	0.79	4.2	4.1	6.5
P_c (10^{-13} yr^{-1})	Jupiter family	0.046	0.22	0.19	0.27
	Saturn family	1.1	5.1	4.5	6.1
δ	Long period	18.3	10.5	8.2	6.1
	Jupiter family	~35	~35	~35	~35
	Saturn family	~35	~35	~35	~35
Γ (10^{-14} $km^{-2}yr^{-1}$)	Long period	0.51	0.30	0.19	0.12
	Jupiter family	0.037	0.011	0.007	0.004
	Saturn family	~1.5	~0.6	~0.3	~0.2
	Total	~2.	~1.	~0.5	~0.3

U = mean dimensionless encounter velocity at sphere of influence of Saturn, weighted by collision probability (U is ratio of encounter velocity to Saturn's mean orbital velocity).

v_i = mean impact velocity, weighted by collision probability.

F = mean enhancement of the flux of comets at the orbital radius of the satellite due to the gravitational field of Saturn, weighted by collision probability.

D = mean diameter of craters created by impacts of 10^{16} g cometary nuclei, weighted by collision probability.

P_c = mean probability of collision of comet.

δ = ratio of cratering rate at apex of satellite's orbital motion to cratering rate at antapex.

Γ = estimated rate of creation of craters 10 km in diameter and larger.

VARIATIONS IN CRATER DENSITIES ON MIMAS, DIONE, AND RHEA. J.B. Plescia, Jet Propulsion Laboratory, Calf. Inst. Technology, Pasadena, 91103, Dept. Geological Sci., Univ. So. Calf., Los Angeles, 90007, and J.M. Boyce, NASA Headquaters, Washington, D.C. 20546.

In order to determine if variations in crater density occur on the surfaces of the Saturnian satellites, preliminary crater counts have been compiled for areas on Mimas, Dione, and Rhea.

Crater counts for Mimas were determined for three areas in the south polar region along the terminator. The cumulative size frequency distributions are illstratede in figure 1 (one of the distriubtions was omitted for purposes of clarity as it lay directly ontop of the two shown). These and additional data suggest that the areas observed on Mimas exhibits a very old and densely cratered surface which has not been subsequently modified. Mimas has a similar size frequency slope as the dark terrain on Ganymede, but a higher overall density.

Dione exhibits several terrains of varying morphology and crater density. We have divided the surface imaged at highest resolution (40° longitude) into three units on the basis of morphology, albedo, and crater density. The units consist of (1) a region of very heavily cratered and rough terrain, (2) an area of plains with intermediate crater density, and (3) lightly cratered plains which are cut by troughs extending from the north pole. Cumulative frequency distributions (figure 2) indicate that the heavily cratered terrain is significantly more cratered than either the plains units or the dark terrain of Ganymede. This heavily cratered area has a lower cumulative frequency slope than the other units and crosses the plains units curves at 10 km. The intersection of curves indicates that more small craters relative to large craters occur on the plains units compared with the heavily cratered terrain. This suggests that some process is operating on the heavily cratered terrain which removes small craters, relative to large ones. Size frequency curves for the plains units are steeper than the heavily cratered terrain and also the dark terrain on Ganymede, indicating a paucity of large craters relative to small craters. Both the lightly and intermediately cratered plains units lack craters larger than 30 km, further suggestive of the relative youth of these surfaces.

The surface of Rhea also exhibits surfaces with different morphologies and crater densities. The north polar region can be divided into two areas; (1) a high albedo region on the trailing hemisphere in which craters larger than 30 km are common, and (2) a low albedo region on the leading hemisphere where craters larger than 30 km are absent. While there is a significant difference in the population of large craters, the density and distribution of small craters is similar for the two areas.

A second type of variation has been noted in the equatorial region of Rhea. Large areas there appear to have been mantled, resulting in the burial of small (less than 20 km) craters. Larger craters remain visible, but are greatly subdued in appearance. The mantling has covered large but discontin-

uous areas of the surface. The effects of this mantling on the cumulative size frequency distribution of craters is illustrated in figure 3. At diameters larger than 20 km no significant difference in density is noted. However at smaller diameters the unmantled area has significantly more craters and a steeper distribution slope than the mantled area.

A crater density gradient from the apex to antiapex of motion has been proposed for the Saturnian satellites (E. Shoemaker, 1981, personal communication; 2), similar to that which occurs on the Galilean satellites (1). Because of the limited longitudinal coverage at high resolution of the Saturnian satellites, this hypothesis is not presently testable, except on Rhea. Sufficent coverage exists for Rhea, but enough crater density determinations have yet to be made to draw any conclusions.

REFERENCES (1) Shoemaker G., and Wolfe, R. (1981) Crater time scales for the Galilean satellites. Submitted to "The Satellites of Jupiter", D. Morrison, ed.; (2) Smith et al. (1981) Encounter with Saturn. in preparation for Science.

This abstract is the result of one phase of research carried out at the Jet Propulsion Laboratory, California Institute of Technology, Pasadena, California, under NASA contract NAS 7-100 sponsored by the National Aeronautics and Space Administration.

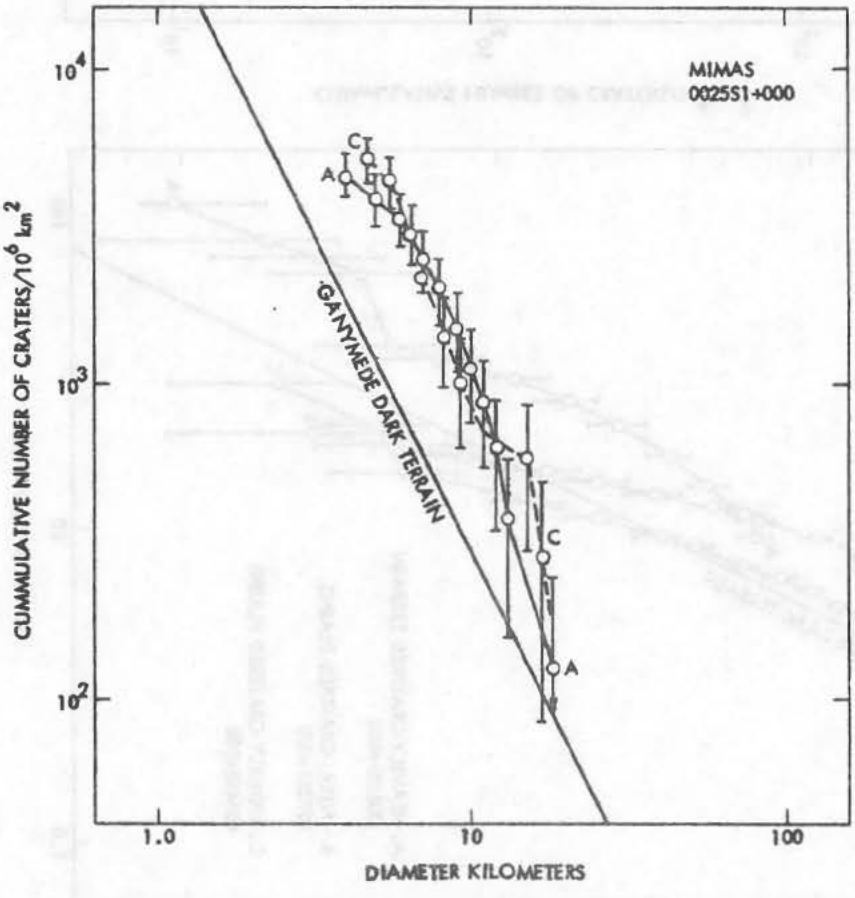

FIGURE 1.

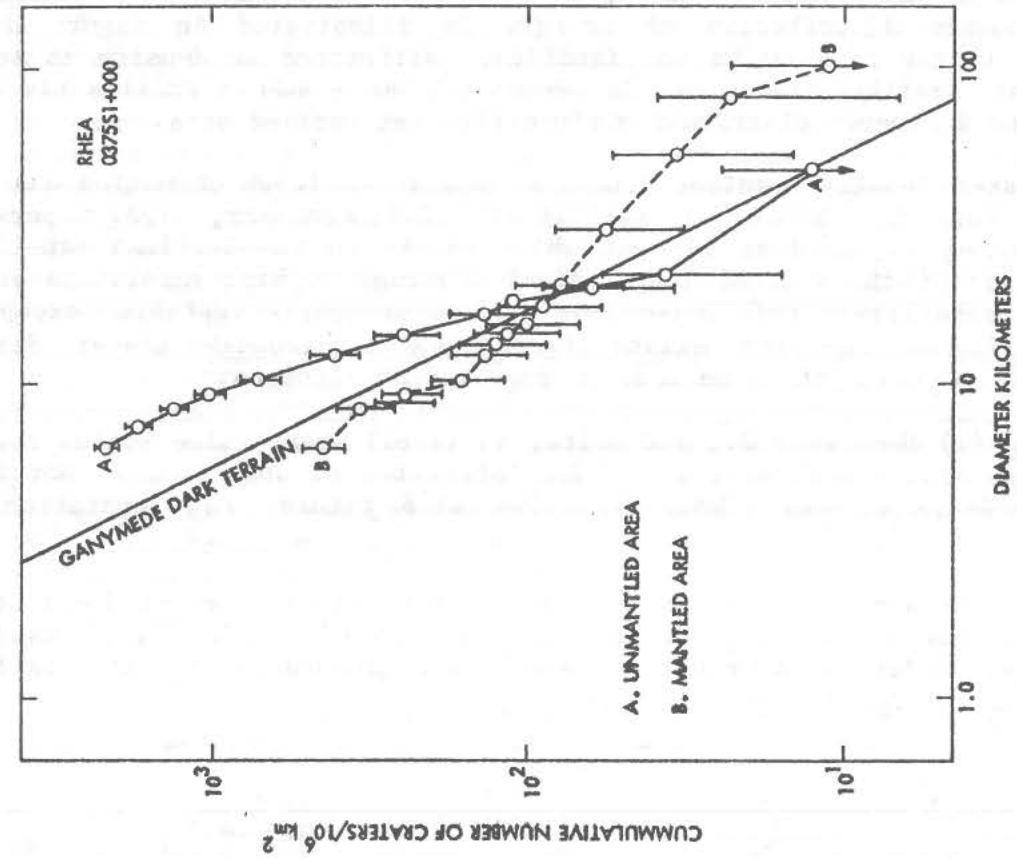

Figure 3

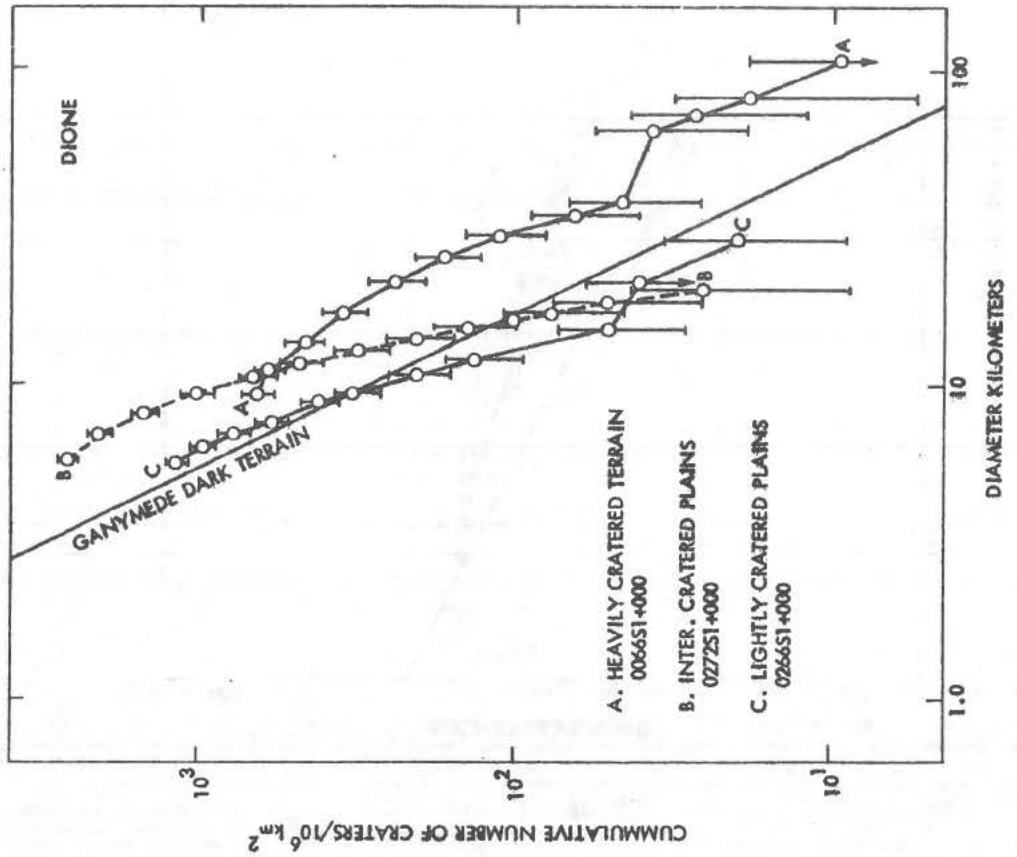

Figure 2

CRATER POPULATIONS ON MIMAS, DIONE AND RHEA. Robert G. Strom, Lunar and Planetary Lab., Univ. of Arizona, Tucson, AZ 85721.

The process responsible for the majority of landforms on Mimas, Tethys, Dione and Rhea has been impact cratering. Although regions of some of these satellites appear to have been resurfaced by internal processes, the main crater degradational process seems to have been subsequent impact. No relaxed craters or palimpsests, such as occur on Ganymede and Callisto, have been observed.

Figure 1 is the crater diameter/density distributions for Mimas, Dione, Rhea and Tethys shown on the relative plot where R is the ratio of the observed distribution to the distribution function $N=D^{-3}$. On this plot a -3 distribution function is a horizontal line and the vertical position represents the relative crater density. Also shown on these plots for comparison is the smoothed average highlands and post-mare lunar crater curves. The crater measurements were compiled over as large an area as possible in order to obtain a statistically meaningful sample at large diameters ($\geq$30 km). For Mimas the craters on the three highest resolution Voyager 1 pictures were counted over a combined area of 5.69×10^4 km^2. The Dione curve represents both heavily and lightly cratered regions displayed on the highest resolution mosaic. The two curves for Rhea represent portions of the north polar leading (area=3.48×10^5 km^2) and trailing (area=1.11×10^4 km^2) hemispheres. Although craters on the highest resolution Voyager 1 image ($\sim$11 km/lp) of Tethys were counted, the data are too poor to determine the shape of the curve. However at diameters of about 30-40 km the crater density appears to be similar to that on Rhea.

The curves for Mimas and Dione show an abundance of craters in the 5-25 km diameter range relative to larger diameters. The maximum crater density occurs at about 10-20 km diameter on both satellites and is about a factor of 4 to 7 times greater than that of the average lunar highlands. In this diameter range Dione has a crater density about a factor of 2 less than Mimas which probably reflects a resurfacing event on Dione represented by the more lightly cratered region. At least on Dione, and possibly Mimas, the curve at larger diameters appears to level out. On Rhea the north polar leading hemisphere has a crater curve which can be represented by a single-slope distribution function of about -2.8 over the diameter range of 5-60 km. No over-abundance of small craters are evident, as occurs on Mimas and Dione. On the measured part of the north polar trailing hemisphere the crater density is greater than the leading hemisphere over the diameter range of 10-30 km, but the slope of the curve is not statistically different from that of the leading hemisphere. However at larger diameters there may be a paucity of craters relative to the leading hemisphere, possibly the result of a resurfacing event.

Figure 2 is a summary plot showing the smoothed curves for Mimas, Rhea (north polar leading hemisphere), and Dione compared with those of the Moon and Callisto. Also shown on this plot, represented by short vertical lines, are the diameters of each of these satellites. These data indicate that at least two families of impacting objects have been responsible for the observed crater distributions; one represented by the -2.8 distribution function displayed by craters on the north polar leading hemisphere of Rhea and by the larger craters on at least Dione, and another later arriving family represented by the smaller crater population (5-25 km) on Mimas and Dione and possibly Rhea. Furthermore the distribution functions of both populations are significantly different from that of the lunar highlands suggesting they represent populations of objects different from that

responsible for the period of heavy bombardment in the inner Solar System. Another indication of differences between the inner and outer Solar System objects is the apparent paucity of large craters on the Saturnian satellites. The largest crater observed on any Saturnian satellite is a 200 km feature on Rhea. If Rhea were capable of sustaining an impact large enough to form a crater 50% its diameter then the crater would be about 700 km in diameter. On the Moon there are about 50 cratersand basins between 200 and 700 km diameter. If the same diameter/frequency distribution of objects impacted Rhea then one might expect about 5 craters of this size range over the 50% of Rhea seen at resolutions adequate to identify such craters. Furthermore, the minimum density in the crater curve for Callisto (Figure 2) occurs at about the same diameter (150 km) as that where Saturnian satellites begin to show a paucity or absence of large craters. This suggests that the paucity of large craters on Callisto may be at least partly due to a paucity of large impacting bodies rather than solely the result of crater obliteration of relaxation in ice. These comparisons suggest that the population of impacting bodies in the outer Solar System was deficient in large bodies relative to that responsible for heavy bombardment in the inner Solar System.

CRATER POPULATIONS

Strom, R. G.

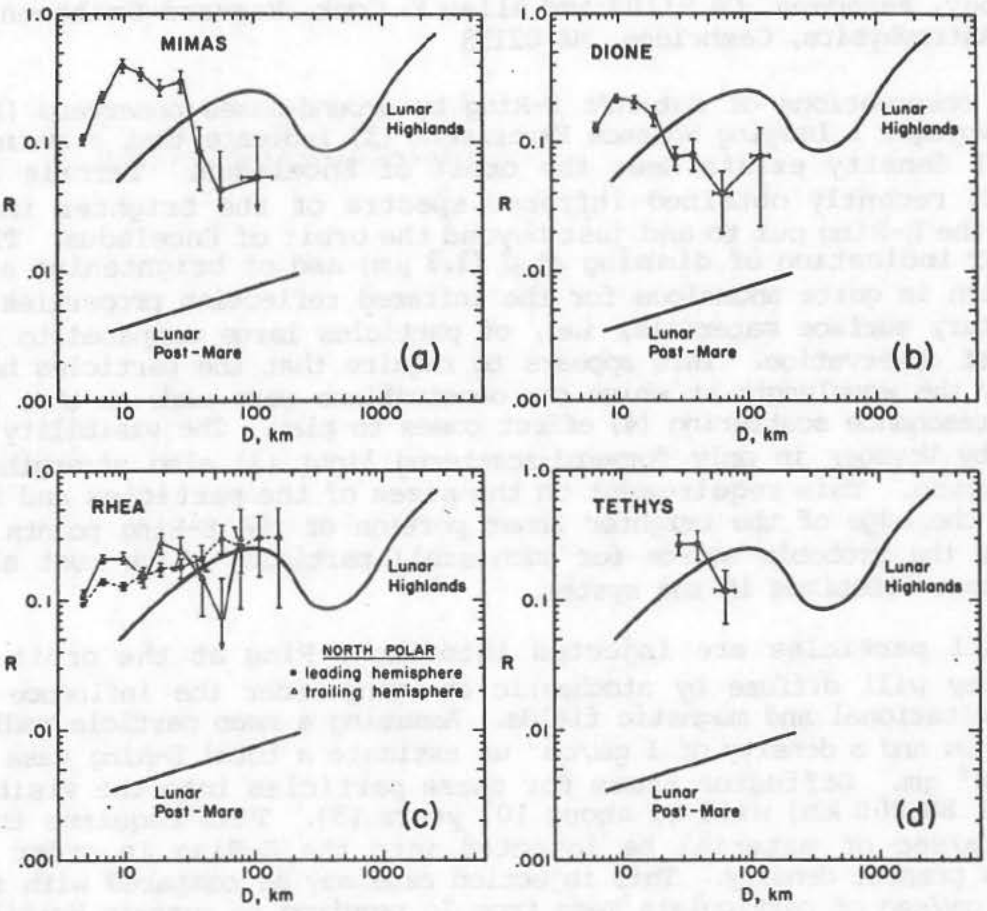

Figure 1

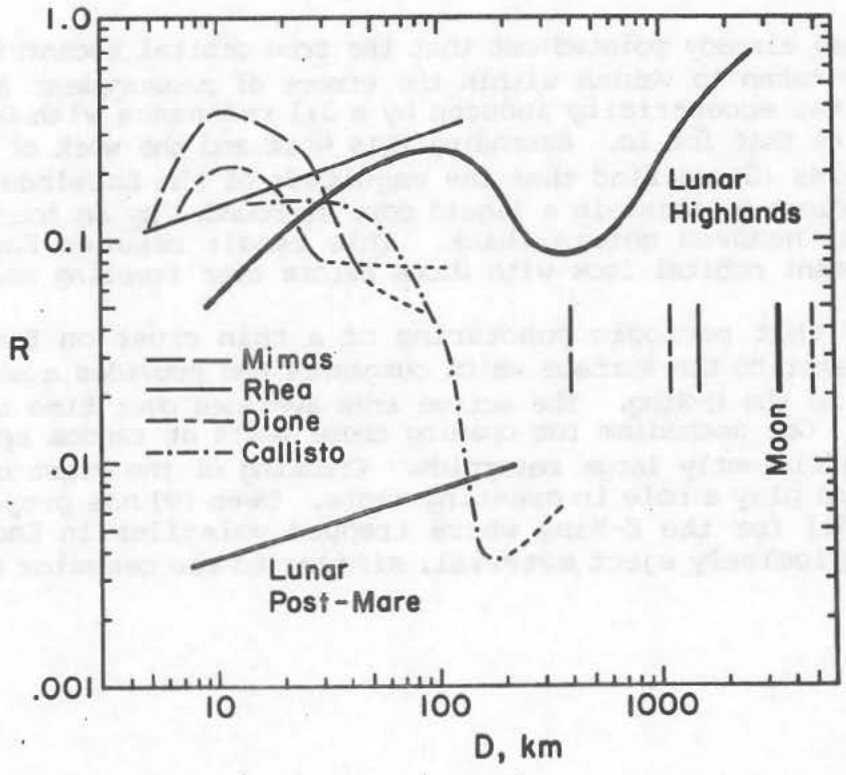

Figure 2

ENCELADUS: EVOLUTION AND POSSIBLE RELATIONSHIP TO SATURN'S E-RING. Richard J. Terrile, Jet Propulsion Laboratory, California Institute of Technology, Pasadena, CA 91103 and Allan F. Cook, Harvard-Smithsonian Center for Astrophysics, Cambridge, MA 02138

Recent observations of Saturn's E-Ring by ground-based observers (1,2) and by the Voyager 1 Imaging Science Experiment (3) indicate that a maximum in material density exists near the orbit of Enceladus. Terrile and Tokunaga (2) recently obtained infrared spectra of the brighter inner portion of the E-Ring out to and just beyond the orbit of Enceladus. They find a clear indication of dimming at J (1.3 μm) and of brightening at K (2.2 μm) which is quite anomalous for the infrared reflection properties of other planetary surface materials, i.e., of particles large compared to the wavelength of observation. This appears to require that the particles have radii nearly the wavelength at which the observations were made so that the well-known resonance scattering (4) effect comes to play. The visibility of the E-Ring by Voyager in only forward-scattered light (3) also strengthens this conclusion. This requirement on the sizes of the particles and the position of the edge of the brighter inner portion of the E-Ring points to Enceladus as the probable source for such small particles which must also have very short lifetimes in the system.

If small particles are injected into the E-Ring at the orbit of Enceladus they will diffuse by stochastic charging under the influence of Saturn's gravitational and magnetic fields. Assuming a mean particle radius of about 2.5 μm and a density of 1 gm/cm^3 we estimate a total E-Ring mass of about 3 x 10^8 gm. Diffusion times for these particles into the visible rings (about 88,000 km) will be about 10^4 years (5). This requires that about 0.1 gm/sec of material be injected into the E-Ring in order to maintain its present density. This injection rate may be compared with the value of 13 gm/sec of particulate mass from Io required to sustain Morfill, Grun and Johnson's (6) model of the Jovian ring.

Yoder (7) has already pointed out that the free orbital eccentricity of Enceladus can be taken to vanish within the errors of measurement and that its forced orbital eccentricity induced by a 2:1 resonance with Dione is almost the same as that for Io. Extending this work and the work of Cassen, Peale and Reynolds (8) we find that the magnitude of the Enceladus tidal heating is sufficient to maintain a liquid core surrounded by an ice or snow crust of several hundred meters thick. This result assumes Enceladus acquired its present orbital lock with Dione before ever freezing solid.

We propose that periodic puncturing of a thin crust on Enceladus exposes liquid water to the surface which outgasses and provides a source of small particles to the E-Ring. The active area averaged over time required is about 50 cm^2. One mechanism for opening these vents at random epochs is by impacts of sufficiently large meteroids. Cracking of the crust by tidal stresses may also play a role in creating vents. Owen (9) has proposed an alternative model for the E-Ring where trapped volatiles in Enceladus periodically explosively eject material, similar to the behavior of some

comets. This model does not require an extremely thin crust and a liquid interior.

Voyager 1 images of Enceladus (3) show a smooth highly reflective surface with no visible topographic features. At similar resolutions craters were observed on all the other icy satellites in the Saturnian system. Our model for the interior of Enceladus predicts a very smooth surface with almost no topography whereas Owen's model calls for blanketed craters and deep fissure topography. Higher resolution observations of this satellite by Voyager 2 should be able to discriminate between current models as well as providing better information on the nature of the E-Ring.

This paper represents one phase of research carried out at the Jet Propulsion Laboratory, California Institute of Technology, under contract NAS 7-100 sponsored by the National Aeronautics and Space Administration.

REFERENCES: (1) Baum W. A. et al. (1980) Bull. Amer. Astro. Soc., 12, 700. (2) Terrile, R. J. and Tokunaga, A. (1980) Bull. Amer. Astro. Soc., 12, 701. (3) Smith, B. A. et al. (1981) Science, in press. (4) van de Hulst, H. C. (1957) Light Scattering by Small Particles, Wiley pub. N.Y., 131-165,209-236. (5) Cook, A. F. and Terrile, R. J. (1981) Nature, submitted. (6) Morfill, G. E. et al. (1981) Planet. & Space Sci. in press. (7) Yoder, C. F. (1979) Nature, 279, 767. (8) Cassen, P. et al. (1979) Geophys. Res. Letter, 6, 731. (9) Owen, T., Nature, submitted.

BULK PROPERTIES OF THE SATURNIAN SATELLITES: IMPLICATIONS FOR EVOLUTION. L. A. Soderblom, United States Geological Survey, Flagstaff, Arizona, and T. V. Johnson, Jet Propulsion Laboratory, California Institute of Technology, Pasadena, California.

Before the Voyager 1 encounter with the saturnian system, it was known from a combination of ground-based and Pioneer-Saturn observations that the densities of the major regular satellites range from 1 to 2 $g \cdot cm^{3}$. Except for Titan, these satellites can be grouped in terms of size into three pairs for ease of comparison: Mimas and Enceladus (400 and 500 km in diameter respectively), Tethys and Dione (about 1,100 km in diameter), and Rhea and Iapetus (about 1,500 km in diameter). Little is known of the bulk properties of the remaining regular satellites.

Before Voyager 1 arrived at Saturn, these satellite densities were not well enough known to determine whether they increase systematically with distance from Saturn, following trends like those of the Solar System as a whole and of the Galilean satellite system. Voyager 1 images have provided close estimates for diameters (Smith et al., 1981) and Voyager 1 radio tracking has improved knowledge of Rhea's mass (Tyler et al., 1981). Densities are now well determined for four of the five inner icy satellites: Mimas, 1.2 $g \cdot cm^{-3}$ Tethys, 1.0 $g \cdot cm^{-3}$ Dione, 1.4 $g \cdot cm^{-3}$; and Rhea, 1.3 $g \cdot cm^{-3}$ (all to an accuracy of better than ± 0.1 $g \cdot cm^{-3}$). The values indicate a crudely outward increasing trend that is consistent with a model (Pollack et al., 1976) in which Saturn was greatly expanded during accretion of the satellites, perhaps beyond Rhea's orbit, owing to its original high internal energy. Silicate gains that condensed early were then cleaned out of the region of the inner satellites' orbits by gas drag. As Saturn lost heat and collapsed, water ice remained as the principal condensing constituent. The innermost satellites would contain the least silicate. Although the observed densities of Mimas, Tethys, Dione, and Rhea are roughly consistent with this predicted increasing density gradient away from Saturn, the densities deviate randomly from this trend beyond the limits of the errors. Mimas is definitely denser than Tethys and Dione is definitely denser than Rhea. Furthermore, Tethys, and Dione are nearly identical in diameter, are close neighbors in their distance from Saturn, and differ most in density among the inner icy satellites. Evidently, the accretion was more complex than a slow continuous process as Saturn's gas envelope shrank; some randomization is implied. Perhaps a process like that described above (Pollack et al., 1976) was involved during an early stage developing the crude density gradient. Evidently, material was later added to the satellite system, probably from external debris in heliocentric orbits. We suggest that these inner satellites are small enough that random variations in the heterogeneous composition of the accreting the planetesimals are recorded in their bulk properties. If so we can place crude limits on the size and composition of the planetesimals themselves. A reasonable range in their densities might be 1 to 3 $g \cdot cm^{-3}$. for the random sample of planetesimals making up a satellite to be small enough to cause the observed variations, the planetesimals would have to be about 100 km or larger in size. Were they much smaller, their variations would simply have been averaged out. If this hypothesis is correct, we have discovered an organized collection of objects small enough to reflect the very nature of accretion itself.

References

Smith, B. A., et al. (1981) Encounter with Saturn: Voyager 1 Imaging Science Results, Science (in press).

Tyler, G. L., et al. (1981) Radio Science Investigations of the Saturn System with Voyager 1: Preliminary Results, Science (in press).

Pollack, J. B., et al. (1976) The Formation of Saturn's Satellites and Rings as Influence by Saturn's Contraction History, Icarus, 29, 35.